Atrial systole enhances intraventricular filling flow propagation during increasing heart rate

Arvind Santhanakrishnan, *Oklahoma State University*
Ikechukwu Okafor, *Georgia Institute of Technology*
Gautam Kumar, *Emory University*
Ajit Yoganathan, *Emory University*

Copyright information:

HHS Public Access

Atrial systole enhances intraventricular filling flow propagation during increasing heart rate

Arvind Santhanakrishnan[1,4,*], **Ikechukwu Okafor**[2], **Gautam Kumar**[3], and **Ajit P. Yoganathan**[2,4]

Arvind Santhanakrishnan: askrish@okstate.edu; Ikechukwu Okafor: iokafor3@gatech.edu; Gautam Kumar: gautam.kumar@emory.edu; Ajit P. Yoganathan: ajit.yoganathan@bme.gatech.edu

[1]School of Mechanical and Aerospace Engineering, Oklahoma State University, 218 Engineering North, Stillwater, OK 74078, USA

[2]School of Chemical and Biomolecular Engineering, Georgia Institute of Technology, Atlanta, GA 30332, USA

[3]Division of Cardiology, Emory University School of Medicine, Atlanta, GA 30322, USA

[4]Wallace H. Coulter Department of Biomedical Engineering, Georgia Institute of Technology & Emory University, 315 Ferst Drive, Atlanta, GA 30332, USA

Abstract

Diastolic fluid dynamics in the left ventricle (LV) has been examined in multiple clinical studies for understanding cardiac function in healthy humans and developing diagnostic measures in disease conditions. The question of how intraventricular filling vortex flow pattern is affected by increasing heart rate (HR) is still unanswered. Previous studies on healthy subjects have shown a correlation between increasing HR and diminished E/A ratio of transmitral peak velocities during early filling (E-wave) to atrial systole (A-wave). We hypothesize that with increasing HR under constant E/A ratio, E-wave contribution to intraventricular vortex propagation is diminished. A physiologic *in vitro* flow phantom consisting of a LV physical model was used for this study. HR was varied across 70, 100 and 120 beats per minute (bpm) with E/A of 1.1–1.2. Intraventricular flow patterns were characterized using 2D particle image velocimetry measured across three parallel longitudinal (apical-basal) planes in the LV. A pair of counter-rotating vortices was observed during E-wave across all HRs. With increasing HR, diminished vortex propagation occurred during E-wave and atrial systole was found to amplify secondary vorticity production. The diastolic time point where peak vortex circulation occurred was delayed with increasing HR, with peak circulation for 120 bpm occurring as late as 90% into diastole near the end of A-wave.

The role of atrial systole is elevated for higher HR due to the limited time available for filling. Our baseline findings and analysis approach can be applied to studies of clinical conditions where impaired exercise tolerance is observed.

Keywords

Intraventricular flow; left ventricle; heart rate; atrial systole; flow phantom

INTRODUCTION

Intraventricular vortex formation during diastole has been examined in multiple studies for providing insight into normal cardiac function and also for diagnostic purposes in diseases such as dilated cardiomyopathy, diastolic dysfunction (DDF) and heart failure with normal ejection fraction (HFNEF) (Eriksson et al. 2011; Gharib et al. 2006; Ghosh et al. 2014; Hendabadi et al., 2013; Kheradvar et al., 2012; Le and Sotiropoulos, 2013; Pedrizzetti et al., 2014; Pedrizzetti et al., 2015; Seo at al., 2014; Stewart et al., 2012). A baseline understanding of exercise hemodynamics for healthy conditions is needed prior to comparison with pathological conditions such as DDF and HFNEF where exercise intolerance is observed (O'Rourke, 2001; Udelson, 2011). The paradigm of intraventricular vortex characterization can be extended for studies of exercise physiology. While hemodynamic characteristics such as pressures, ejection fraction, E/A ratio and E/E′ ratio have been examined under increasing heart rate (HR) for healthy volunteers (Iliceto et al., 1991; Swinne et al., 1992; Yamamoto et al., 1993), no study to date has examined the alterations in intraventricular filling flow patterns under increased HR. This latter point is the subject of the current study.

We use physical modeling to address a basic but unanswered question: how does increasing HR impact intraventricular filling when E/A ratio and systemic pressure are maintained constant? Though the latter assumptions are not truly reflective of the hemodynamic alterations that typically occur during exercise (increased SV, pulse pressure and E/A ratio), we underscore that our current effort is the starting point to tackle a complex physiological scenario in a systematic manner. Clinical studies of exercise hemodynamics under increasing HR are challenged in their ability to provide mechanistic explanations for functional observations, mainly due to highly interrelated nature of the underlying physiological variables (e.g., age, sex, systemic pressure, SV, LV stiffness, pulmonary venous flow, venous return). Physical models such as what was used in this study can provide a powerful means to examine the isolated mechanistic impact of select variables on specific hemodynamic and functional outcomes in physiological studies.

We hypothesize that with increasing HR under constant E/A ratio, the contribution of the E-wave to the propagation of intraventricular filling flow is diminished. We expect this based on the limited overall diastolic duration with increasing HR. We tested the hypothesis using an *in vitro* LV phantom model. The rationale for maintaining a constant E/A across all conditions was to identify if there were any changes in intraventricular flow simply due to increasing HR, even when contribution of atrial systole (hereon referred to as A-wave)

relative to early diastolic filling (hereon referred to as E-wave) remains unaltered from resting condition.

MATERIALS AND METHODS

In Vitro Flow Circuit

A programmable piston-driven left heart simulator (LHS) was used to study the blood flow characteristics within the ventricle (Fig. 1a). The LHS consists of an atrium, a flexible and transparent LV, an aorta, and adjustable systemic compliance and resistances, enabling physiological pressure and flow conditions to be achieved. The piston pump alters the pressure in the outer chamber housing the ventricle, causing it to expand/contract and thereby driving the blood flow within the LV. More details on the LV model design and flow circuit can be found elsewhere (Okafor et al., 2015). A bileaflet mechanical heart valve (BMHV) was placed at the aortic annular plane. A D-shaped mitral annulus was used without valve leaflets to minimize valvular artifacts and resulting disturbances to the intraventricular flow field. A bi-leaflet mechanical heart valve was used upstream of the mitral annulus (closer to the atrial reservoir) to simply ensure unidirectionality of flow through the *in vitro* flow circuit. The geometric area of the mitral orifice was 3.0 cm^2. The mean aortic pressure was set to 100 mm Hg at a cardiac output of 4.2 L/min. A solution of water-glycerin (36% by volume glycerin) was used to match the viscosity and density of blood (3.5 cP and 1.08 g/cm^3, respectively). The E-wave maximum for the mitral inflow was set at ~15 L/min while the A-wave maximum was set at ~13 L/min (standard deviation of +/− 0.35 L/min). The E/A ratio, calculated as peak E-wave flow rate divided by peak A-wave flow rate, was maintained constant in the range of 1.1–1.2 across all experiments in this study. A-wave was generated by retracting the programmable piston pump a second time, after a brief pause in the piston motion. The input voltage waveform for the programmable piston pump (PPP, Fig. 1b) was adjusted across each HR case to obtain roughly equivalent mitral flow rate curves as shown in Fig. 2.

Experimental Conditions

Three HRs were studied: 70, 100, and 120 bpm. The length of the diastolic period was calculated using the empirical relationship described by Cui and Roberson (2006). Table 1 shows the characteristics for each HR condition tested in this study.

Particle Image Velocimetry (PIV) Setup

Phase locked 2D PIV was used to observe the instantaneous flow fields at 3 longitudinal planes in the LV: center plane, and 2 others d/2 to the left and right of the center plane, where d is the hydraulic diameter of the mitral orifice. Figure 1c shows the schematic of the PIV setup. The thickness of the laser sheet was roughly 1 mm. The resolution of the PIV camera was 1600×1200 pixels with the particle image size ranging between $2 – 3$ pixels. 200 image pairs were acquired at $25 – 35$ phases (depending on heart rate) during the diastolic period of the cardiac cycle. DaVis 7.2 software (LaVision GmbH, Göttingen, Germany) was used to perform dual-pass cross correlation with decreasing window size (64 $\times$ 64 to 32 $\times$ 32 pixels; 50% overlap each). A sliding background subtraction of a scale

length of 5 pixels was used to preprocess the raw images. A median filter was implemented to erase noisy vectors; interpolation was then performed to fill up empty spaces.

Hemodynamic parameters

The following hemodynamic parameters were calculated from the experimental data obtained using flow probes and pressure transducers:

$$SV = EDV - ESV \quad (1)$$

$$EF\,[\%] = 100 \times \frac{SV}{EDV} \quad (2)$$

$$Wo = D.\sqrt{\frac{2\pi f}{\nu}} \quad (3)$$

where: *SV* is the stroke volume (in mL/beat), *EDV* is the end diastolic volume (in mL), *ESV* is the end systolic volume (in mL), *EF* is the ejection fraction (in %), *Wo* is the Womersley number (non-dimensional ratio of pulsatility in flow to viscous effects), *D* is the mitral annulus diameter (in meters), *f* is the heart rate (in beats/s), and ν is the kinematic viscosity of the blood analog solution (in m^2/s).

Vortex Formation Time (VFT)

VFT is a non-dimensional index that is commonly used to characterize vortex rings and has been used previously in clinical studies of diastolic filling (Gharib et al., 2006). VFT was calculated based on the relationship proposed by Gharib et al. (2006), as described below:

$$VFT = \frac{4}{\pi D^3}[(EF.EDV) - V_A] \quad (4)$$

where: *D* is the mitral annulus diameter, *EF* is the ejection fraction, and V_A is the portion of the stroke volume contributed by atrial systole.

Vorticity

At each measurement phase and for all HR, the two-dimensional out-of-plane component of the vorticity field was extracted from the velocity measurements. The vorticity field describes the tendency of the fluid to rotate and is mathematically defined as the curl of the velocity field. The out-of-plane vorticity of the flow field was calculated using the following equation:

$$\vec{\omega_z} = \nabla \times \vec{\nu} = \frac{\delta \nu_y}{\delta x} - \frac{\delta \nu_x}{\delta y} \quad (5)$$

Vortex Identification and Circulation

The circulation of the vortex proximal to the aorta was calculated based on the equation:

$$\Gamma = \int_0^A \overrightarrow{\omega_z} \mathrm{dA} \quad (6)$$

where: *A* is the area enclosed within the vortex. Identification of the vortex was performed using the swirling strength λ_{ci}, which is the imaginary part of the complex eigenvalue of the velocity gradient tensor, ∇U. This criterion was used with a 4.2% threshold of the maximum value as proposed by Zhou et al. (1999). This relationship can be approximated for a two-dimensional flow field, as described below (see Adrian et al., 2000, for more details):

$$\lambda_{ci} = Im[\,eig(\nabla U)\,] = \frac{1}{2}Im\left(\sqrt{\left(\frac{du}{dx} - \frac{dv}{dy}\right)^2 + 4 \cdot \frac{du}{dy} \cdot \frac{dv}{dx}}\right) \quad (7)$$

RESULTS

Hemodynamic parameters

Table 1 shows the hemodynamic parameters calculated using equations (1)–(3). As the peak flow rates for the early filling phase (E-wave) and atrial systolic phase (A-wave) were maintained constant across HR for the study protocols, we observed a reduction in both *SV* and *EF* with increasing HR. This is not observed physiologically, and is due to the inability of the material used in our physical model to alter contractility under increasing HR conditions unlike myocardial tissue. *EDV* was approximately the same across all HR and *ESV* increased with increasing HR. We expected *EDV*. The Womersley number *Wo* increased with increasing HR, which was expected due to the frequency dependence. The *VFT* value for resting HR in our model was above the physiological range of 3.5–5.5 reported by Gharib et al. (2006). This discrepancy was most likely due to the shape and wall stiffness of our LV physical model. The *VFT* value decreased with increasing HR, which was expected due to the reduction of *EF* with increasing HR, as well as increased contribution of atrial systolic volume to the SV (*V_A* term in equation (4)) with increasing HR.

Intraventricular vorticity patterns

The inflow vortex ring at peak E-wave is observed in the central PIV plane for all HR as a pair of counter-rotating, opposite signed vortices. The vortex ring propagation into the LV during E-wave deceleration at resting HR is similar to physiological observations in human LV by Stewart et al. (2012). The shear flow generated by the mitral vortex ring in E-wave decreases with increasing HR, as observed in the longitudinal penetration in the x-direction (Fig. 3(a), (d), and (g)). The penetration of the shear flow toward the apex, engendered by the advecting vortex ring, is most pronounced for resting HR (Fig. 3(b)). This is due to the large value of *VFT* noted previously (longer jet). The E-wave vortex ring propagation is delayed for increased HR cases in comparison (Fig. 3(e) and (h)) due to the shorter time period available for early relaxation phase of filling. A secondary pair of counter-rotating vortices is observed close to the base of the LV model during peak A-wave for resting HR (Fig. 3(c)). In contrast, the peak A-wave phase generates a stronger vortex-laden flow for increased HR (Figs. 3(f) and (i)). Interaction of primary and secondary vortices is seen

during A-wave portion of filling for 100 bpm and 120 bpm (see Figs. 3(f) and (i) at x = 10–40 mm).

Circulation variation with HR

Circulation was evaluated using equation (6) to quantitatively compare intraventricular vortex formation and propagation. The results shown in Fig. 4 were obtained by tracking the vortex proximal to the septal wall of the LV. Overall, the peak value of circulation decreases with increasing HR (Fig. 4(a)). Circulation was normalized for each HR using its local maximum value, and plotted as a function of normalized diastolic time $t_d^* = t/T$ (Fig. 4(b)). Note that t_d^* of roughly 0.5 corresponds to the onset of atrial systole in all HR cases (Fig. 2). Normalized circulation diminishes with increasing filling time under resting HR (Fig. 4(b)). The 120 bpm case shows an opposite trend, with noticeable rise in circulation during the A-wave ($t_d^* > 0.5$). With increasing HR from 100 bpm to 120 bpm, circulation is intensified during A-wave. Maximum normalized circulation occurs later in time with increasing HR, with the 120 bpm case registering peak circulation at $t_d^* = 0.9$, compared to $t_d^* = 0.3$ for 70 bpm and $t_d^* = 0.4$ for 100 bpm.

DISCUSSION

The objective of the current study was to investigate the isolated effect of increasing HR on intraventricular filling flow patterns. Several previous studies conducted *in vivo* have reported a physiological reduction in E/A with increasing HR in healthy subjects (Iliceto et al., 1991; Swinne et al., 1992; Yamamoto et al., 1993). Increasing HR has been correlated to increased atrial systolic velocity (Channer and Jones, 1989; Harrison et al., 1991; Mitchell et al., 1965; Ruskin et al., 1970). However, the functional implication of the elevated role of atrial systole during LV filling under increasing HR is unclear. We hypothesized that with increasing HR under constant E/A ratio, the E-wave contribution to intraventricular filling flow propagation is diminished. Our results indicate that the limited diastolic time available with increasing HR results in diminished circulation of the E-wave filling vortex compared to resting condition. The A-wave portion of the inflow serves to compensate filling through secondary vortex generation, introducing an influx of additional momentum into the LV. The time point in diastole where peak circulation occurs is delayed with increasing HR due to the reduction in filling duration for increased HR.

Our results are supported by measurements of intraventricular flows in healthy humans at resting conditions (Eriksson et al., 2011) where atrial systolic contribution to inflow augmented end-diastolic kinetic energy. The increased circulation during atrial systole could aid in pulling more fluid from the atrium, thereby augmenting the momentum influx as HR increases. Our study shows that the A-wave portion does not impact resting HR as drastically. This is due to the enhanced propagation of shear flow into the LV during E-wave (Fig. 4(a)), resulting in the bulk of intraventricular filling already occurring prior to onset of A-wave. This has also been observed clinically as mitral valve closure following the E-wave due to decreased transmitral bulk flow.

The findings of our study provides a baseline physiological understanding that could be used in future studies to understand the functional implications of physiologically observed

enhancement in atrial systolic contribution and reduced E/A ratio with increasing HR. From a clinical standpoint, our observations could potentially encourage using stress testing and progressive non-invasive monitoring of filling flow patterns in patients that are clinically asymptomatic candidates for HFNEF.

Limitations

Though clinical studies examining exercise hemodynamics with increasing HR show a reduction in E/A ratio, the E- and A-wave portions and peak velocities were maintained nearly constant across all HR tested in this study. This simplification was performed to ensure that the inertial force imparted to the LV flow field by the pulsatile mitral inflow was constant across all HRs (Reynolds number matching across HR). Physiological reduction in E/A with increasing HR, due to increased A-wave peak velocity, will amplify our findings specific to the role of A-wave. Future studies that explore the amplified effect of reduced E/A and increased A-wave peak velocity will aid in furthering our understanding of exercise-induced alterations to intraventricular filling fluid dynamics. Overlapping E- and A-waves were not included in our filling flow profiles at increased HR to demarcate contributions of E- and A-waves to the intraventricular flow. Although pulse pressure increases with exercise (Heidorn, 1958), we maintained a pulse pressure of 40 mm Hg across all HR to ensure that altering afterload did not noticeably alter diastolic LV wall motion. We used an open mitral valve orifice in the mitral annulus for this study to not include potential changes in leaflet fluttering under increasing HR. A previous study examining LV fluid mechanics under varying mitral valve design (Pierrakos and Vlachos, 2006) observed that the filling vortex circulation was altered due to fluttering of leaflets. While the absence of mitral valve leaflets is non-physiological, it allowed us to examine the changes to the filling vortex circulation with increasing HR independent of valve design. Future studies examining mitral valve leaflet fluttering behavior with increasing HR, as well as a larger range of HR than what was investigated in this study, are needed for enabling clinical translation of our study results.

Acknowledgments

References

Adrian RJ, Christensen KT, Liu Z. Analysis and interpretation of instantaneous turbulent velocity fields. Experiments in Fluids. 2000; 29:275–290.

Channer KS, Jones JV. The contribution of atrial systole to mitral diastolic blood flow increases during exercise in humans. The Journal of Physiology. 1989; 411:53–61. [PubMed: 2614731]

Cui W, Roberson D. Left ventricular Tei index in children: comparison of tissue Doppler imaging, pulsed wave Doppler, and M-mode echocardiography normal values. Journal of the American Society of Echocardiography. 2006; 19:1438–1445. [PubMed: 17138026]

Eriksson J, Dyverfeldt P, Engvall J, Bolger AF, Ebbers T, Carlhäll CJ. Quantification of presystolic blood flow organization and energetics in the human left ventricle. American Journal of Physiology - Heart and Circulatory Physiology. 2011; 300:H2135–2141. [PubMed: 21421820]

Gharib M, Rambod E, Kheradvar A, Sahn DJ, Dabiri JO. Optimal vortex formation as an index of cardiac health. Proceedings of the National Academy of Sciences of the United States of America. 2006; 103:6305–6308. [PubMed: 16606852]

Ghosh E, Caruthers SD, Kovacs S. E-wave generated intraventricular diastolic vortex to L-wave relation: model-based prediction with in-vivo validation. Journal of Applied Physiology. 2014; 117:316–324. [PubMed: 24903922]

Harrison MR, Clifton GD, Pennell AT, DeMaria AN. Effect of heart rate on left ventricular diastolic transmitral flow velocity patterns assessed by Doppler echocardiography in normal subjects. American Journal of Cardiology. 1991; 67:622–627. [PubMed: 2000796]

Heidorn GH. Pulse pressure response to a standard exercise stress. Circulation. 1958; 18:249–255. [PubMed: 13561495]

Hendabadi S, Bermejo J, Benito Y, Yotti R, Fernández-Avilés F, del Álamo JC, Shadden SC. Topology of blood transport in the human left ventricle by novel processing of Doppler echocardiography. Annals of Biomedical Engineering. 2013; 41:2603–2616. Epub 2013 Jul 2. 10.1007/s10439-013-0853-z [PubMed: 23817765]

Iliceto S, D'Ambrosio G, Marangelli V, Amico A, Di Biase M, Rizzon P. Echo-Doppler evaluation of the effects of heart rate increments on left atrial pump function in normal human subjects. European Heart Journal. 1991; 12:345–51. [PubMed: 2040316]

Kheradvar A, Assadi R, Falahatpisheh A, Sengupta PP. Assessment of transmitral vortex formation in patients with diastolic dysfunction. Journal of the American Society of Echocardiography. 2012; 25:220–227. [PubMed: 22099070]

Le TB, Sotiropoulos F. Fluid-structure interaction of an aortic heart valve prosthesis driven by an animated anatomic left ventricle. Journal of Computational Physics. 2013; 244:41–62. [PubMed: 23729841]

Mitchell JH, Gupta DN, Payne RM. Influence of atrial systole on effective ventricular stroke volume. Circulation Research. 1965; 17:11–18. [PubMed: 14302547]

Okafor I, Santhanakrishnan A, Chaffins BD, Mirabella L, Oshinski JN, Yoganathan AP. Cardiovascular magnetic resonance compatible physical model of the left ventricle for multi-modality characterization of wall motion and hemodynamics. Journal of Cardiovascular Magnetic Resonance. 2015:17. [PubMed: 25885056]

O'Rourke MF. Diastolic heart failure, diastolic left ventricular dysfunction and exercise intolerance. Journal of the American College of Cardiology. 2001; 38:803–805. [PubMed: 11527637]

Pedrizzetti G, La Canna G, Alfieri O, Tonti G. The vortex--an early predictor of cardiovascular outcome? Nature Reviews Cardiology. 2014; 11:545–553. Epub 2014 Jun 3. 10.1038/nrcardio. 2014.75

Pedrizzetti G, Martiniello AR, Bianchi V, D'Onofrio A, Caso P, Tonti G. Cardiac fluid dynamics anticipates heart adaptation. Journal of Biomechanics. 2015; 48(2):388–391. Epub 2014 Dec 9. 10.1016/j.jbiomech.2014.11.049 [PubMed: 25529139]

Pierrakos O, Vlachos P. The effect of vortex formation on left ventricular filling and mitral valve efficiency. Journal of Biomechanical Engineering. 2006; 128:527–539. [PubMed: 16813444]

Ruskin J, McHale PA, Harley A, Greenfield JC Jr. Pressure-flow studies in man: effect of atrial systole on left ventricular function. The Journal of Clinical Investigation. 1970; 49:472–478. [PubMed: 5415675]

Seo JH, Vedula V, Abraham T, Lardo AC, Dawoud F, Luo H, Mittal R. Effect of the mitral valve on diastolic flow patterns. Physics of Fluids. 2014; 26:121901–14.10.1063/1.4904094

Stewart KC, Charonko JC, Niebel CL, Little WC, Vlachos PP. Left ventricular vortex formation is unaffected by diastolic impairment. American Journal of Physiology - Heart and Circulatory Physiology. 2012; 303:H1255–H1262. [PubMed: 22961866]

Swinne CJ, Shapiro EP, Lima SD, Fleg JL. Age-associated changes in left ventricular diastolic performance during isometric exercise in normal subjects. American Journal of Cardiology. 1992; 69:823–826. [PubMed: 1546666]

Udelson JE. Heart failure with preserved ejection fraction. Circulation. 2011; 124:e540–e543. [PubMed: 22105201]

Yamamoto K, Masuyama T, Tanouchi J, Doi Y, Kondo H, Hori M, Kitabatake A, Kamada T. Effects of heart rate on left ventricular filling dynamics: assessment from simultaneous recordings of pulsed Doppler transmitral flow velocity pattern and haemodynamic variables. Cardiovascular Research. 1993; 27:935–941. [PubMed: 8221781]

Zhou J, Adrian RJ, Balachandar S, Kendall TM. Mechanisms for generating coherent packets of hairpin vortices in channel flow. Journal of Fluid Mechanics. 1999; 387:353–396.
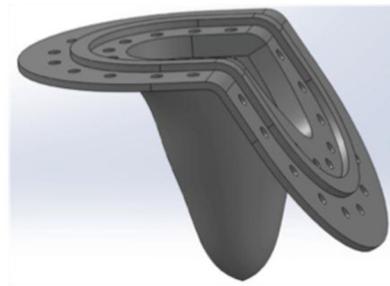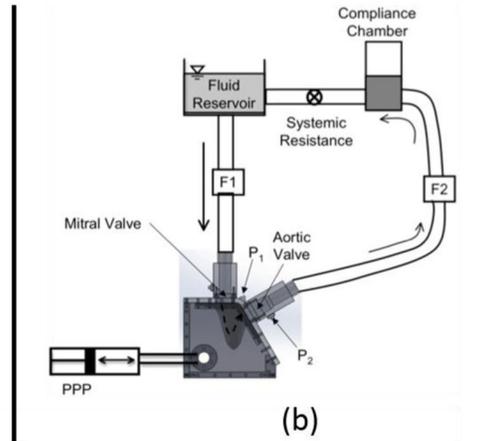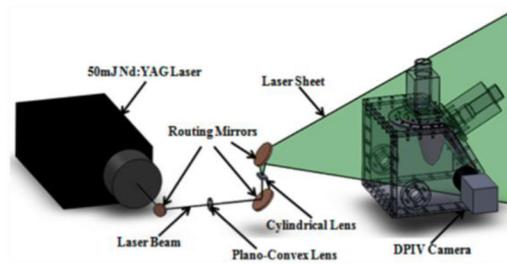
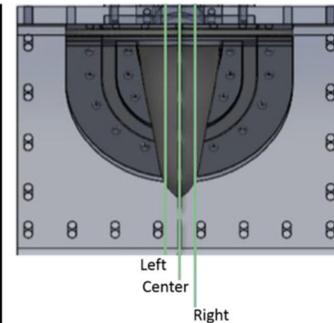**Figure 1.**
Schematic of: (a) LV physical model, and (b) *in vitro* flow circuit used in the study. PPP indicates programmable piston pump. F1 and F2 indicate the locations of mitral and aortic flow probe, respectively. P1 and P2 indicate the locations of LV and aortic pressure transducers, respectively. A bi-leaflet mechanical heart valve was located upstream of the mitral annulus to decouple the role of valve leaflets in this study. (c) Experimental setup used for PIV measurements. (d) The laser sheet was positioned along 3 different planes (marked as left, right and center) to obtain a quasi-3D representation of the flow characteristics during diastole.
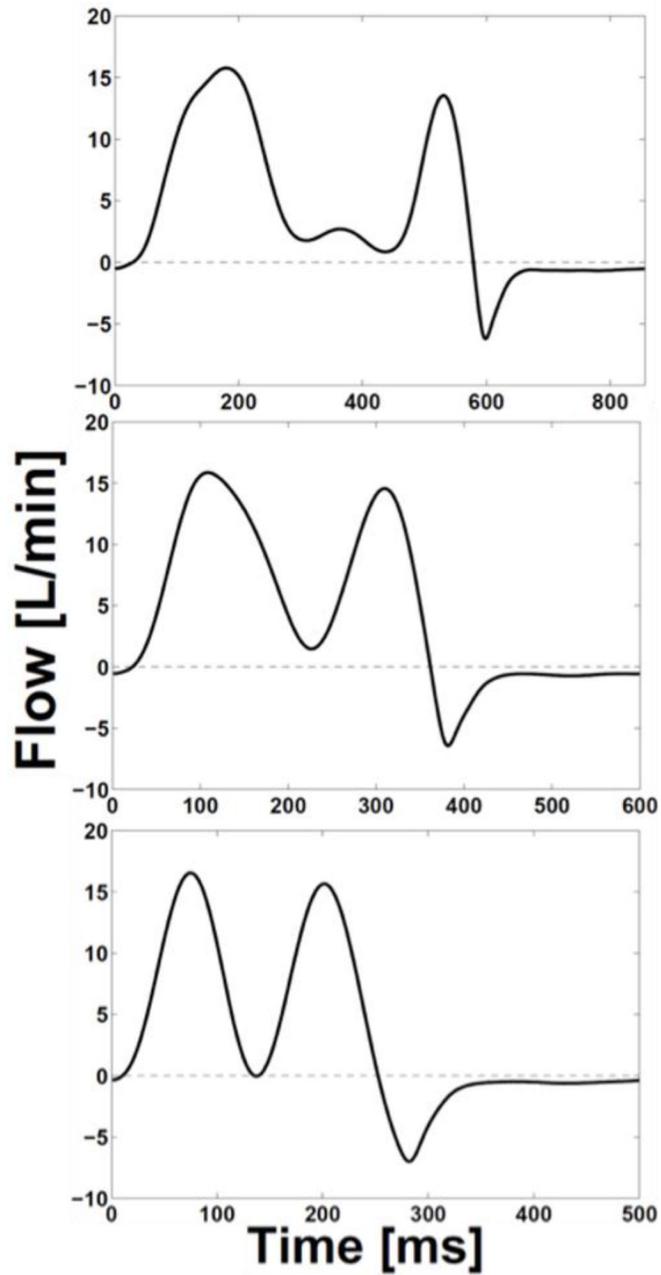
Figure 2.
Mitral inflow curves for 70 bpm (top), 100 bpm (middle) and 120 bpm (bottom) showing biphasic E-wave and atrial systolic peaks.
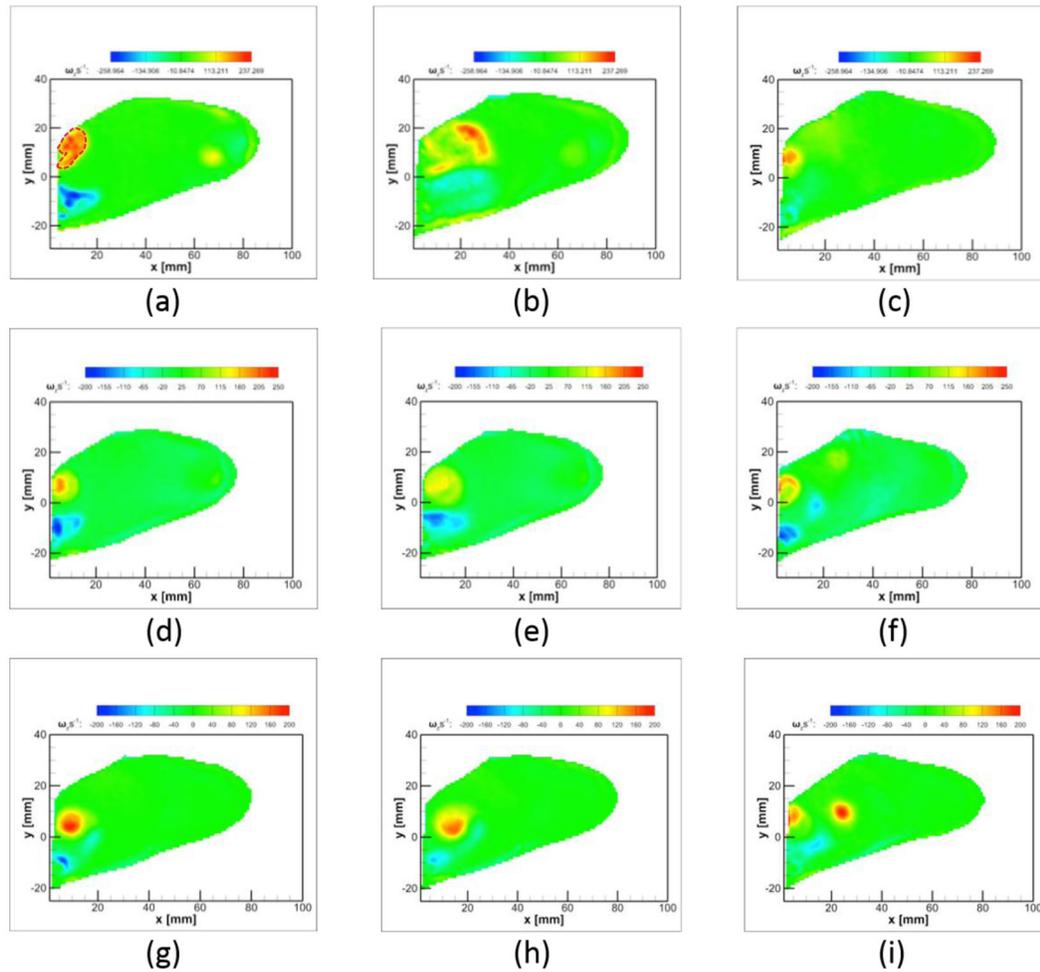
Figure 3.
Basic flow field during three phases of diastolic filling shown via vorticity contours across all three HR. (a) – (c) correspond to 70 bpm, (d) – (f) correspond to 100 bpm, and (g) – (i) correspond to 120 bpm. (a), (d), and (g) were obtained during peak of E-wave in filling. (b), (e), and (h) were obtained during deceleration of E-wave. (c), (f), and (i) were obtained during peak of A-wave. The red boundary in (a) identifies the vortex which was analyzed in this study.
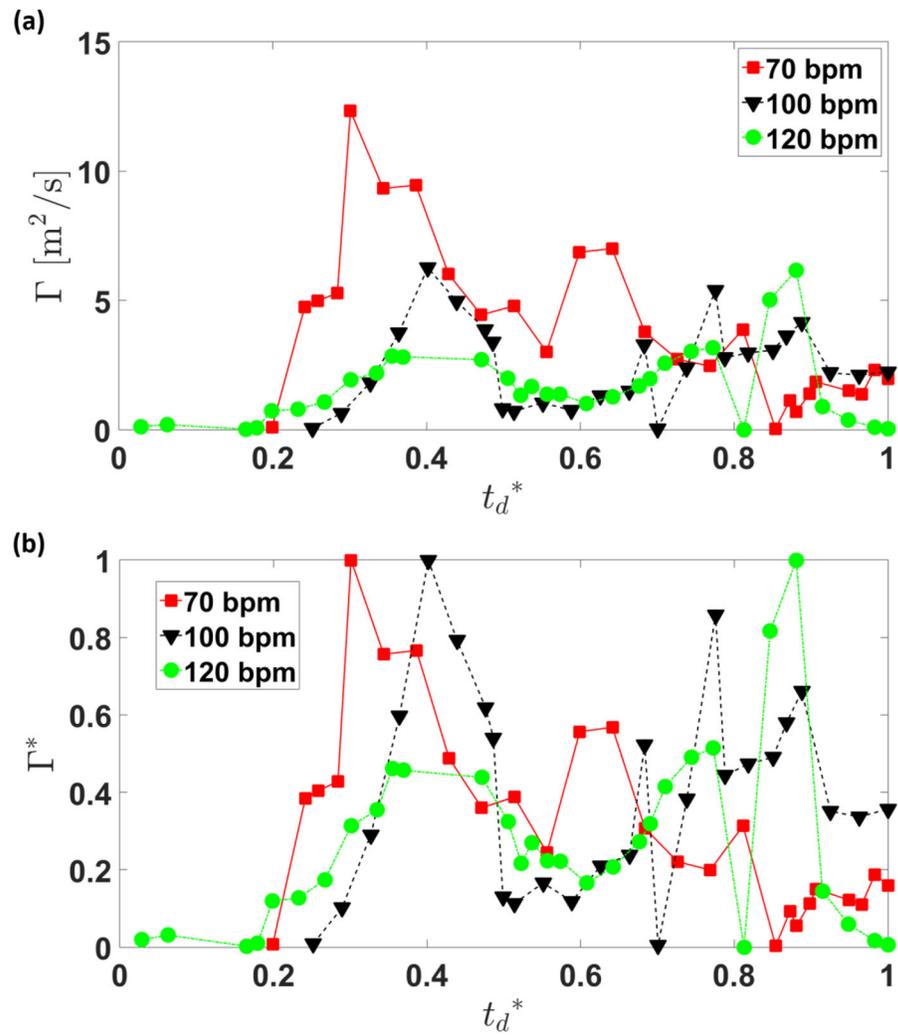
Figure 4.
(a) CS of anterior vortex Γ^* for each HR as a function of non-dimensional diastolic time t_d^*.
(b) Normalized CS with respect to local maximum value. The occurrence of the first peak in CS is shifted further in time with increasing HR.

Table 1

Experimental conditions investigated in the study, including HR (in bpm), time period T of the cardiac cycle (in ms), E/A ratio, and diastolic portion of the total cycle (in %). The systemic pressures for all three conditions were identically tuned to 120/80 mm Hg. Wo = Womersley number; SV = stroke volume; EDV = end diastolic volume; ESV = end systolic volume; EF = ejection fraction; VFT = vortex formation time

HR [bpm]	T [ms]	E/A	% Diastole	Wo	SV [mL/beat]	EDV [mL]	ESV [mL]	EF [%]	VFT
70	856	1.2	66	29.2	64.5	134	65	48.1	8.1
100	600	1.1	58	34.9	48.8	134.5	80	36.3	5.1
120	500	1.1	55	38.2	35.5	130	91	27.3	3.2